Twisted Intramolecular Charge Transfer States in 2-Arylbenzotriazoles: Fluorescence Deactivation via Intramolecular Electron Transfer Rather Than Proton Transfer

Ashok Maliakal,[†] George Lem,[†] Nicholas J. Turro,*[,†] Ravi Ravichandran,[‡] Joseph C. Suhadolnik,[‡] Anthony D. DeBellis,[‡] Mervin G. Wood,[‡] and Jacqueline Lau[‡]

Department of Chemistry, Columbia University, 3000 Broadway, New York, New York 10027, and Ciba Specialty Chemicals, 540 White Plains Road, Tarrytown, New York 10591

Received: April 18, 2002; In Final Form: June 18, 2002

Ultraviolet absorbers such as Tinuvin P (2-(2-hydroxy-5-methylphenyl)benzotriazole), **1**, achieve their exceptional photostabilities as a result of deactivation of excited singlet states through excited state intramolecular proton transfer (ESIPT). Adding a methyl group to the 6′ position of 2-arylbenzotriazoles reveals an additional excited singlet state deactivation mechanism in this class of molecules which does not require intramolecular hydrogen bonding. Steady state fluorescence and fluorescence lifetime measurements for a series of 6′-methyl-2-arylbenzotriazoles provides compelling evidence for a twisted intramolecular charge transfer (TICT) mechanism of excited singlet state deactivation. Due to the steric requirements of the 6′-methyl group, conformations are favored in which the phenyl and triazole rings are no longer coplanar. In the case of compound **11** (2-(6-methoxy-2,3-dimethylphenyl)-2*H*-benzotriazole), the presence of a 2′-methoxy group enhances nonplanarity and results in large deactivation rates. Compound **12** (2-(6-methoxy-2,3-dimethylphenyl)-5-(trifluoromethyl)-2*H*-benzotriazole), which possesses both twist and enhanced donor/acceptor properties, undergoes the most efficient fluorescence quenching for the methoxyarylbenzotriazoles. Compounds with both a 6′-methyl and a hydroxy group on the phenyl ring exhibit diffusion controlled quenching ($k_q = 2 \times 10^{10}$ M^{-1} s^{-1}) by DMSO. This quenching appears to result from either partial or complete excited state proton transfer to DMSO, which enhances TICT deactivation of the singlet excited state.

Introduction

The ability of certain classes of compounds to rapidly dissipate excited state energy without irreversible photochemistry is a requirement for useful ultraviolet absorbers (UVAs). These compounds have exceptional photostabilities with extremely small quantum yields of decomposition (10^{-6} or less).[1−3] One class of such compounds is the 2-(2′-hydroxyaryl)benzotriazoles, of which Tinuvin P (**1**) is a member (see Figure 1). Compound **1** has a very efficient pathway for deactivation of S_1 so that other excited state processes [i.e., intersystem crossing (ISC), fluorescence, photoreaction] are unable to compete (see Scheme 1).[4,5]

The mechanism of fluorescence deactivation of **1** and related compounds has been the focus of several studies,[5−12] whose findings have converged on an excited state intramolecular proton transfer mechanism (ESIPT) of fluorescence deactivation. This mechanism is illustrated in Scheme 1. The excited singlet state is capable of relaxing within ∼100 fs, via adiabatic transfer of the phenolic proton to the nitrogen of the triazole ring producing isomer **K**.[13] The excited state isomer **K**, shows very weak red shifted fluorescence under special conditions;[4,9,11,14−18] however, subpicosecond internal conversion[13] from the excited "keto" form is the strongly favored process.[9]

The ESIPT mechanism has definite conformational requirements, the most important of which is a planar conformation (closed form) that is capable of producing an intramolecular hydrogen bond in the ground state. When the hydrogen bond is broken (open form), the ESIPT deactivation mechanism is lost and the onset of both fluorescence and photoreactivity (loss of stability) is observed.[10,12,19,20] Thus, a paradigm has developed which teaches that the best benzotriazole UVAs require both coplanarity and a strong intramolecular hydrogen bond. Indeed, parallels between intramolecular hydrogen bond strength and performance as a UVA have been suggested as a means for more efficient evaluation of promising lead compounds for improved UVAs.[11,14,21]

Other mechanisms for ultrafast deactivation, such as twisted intramolecular charge transfer (TICT),[22,23] have been exploited in applications such as laser dye absorbers used in mode-locked lasers.[24] In the TICT mechanism, rotation around a bond connecting a donor group and an acceptor group can decouple the orbitals of these two groups. This orbital decoupling provides a means by which nearly complete electron transfer from the donor to the acceptor can occur.[25] A highly polar twisted excited state results which, under appropriate solvent conditions, can be preferentially stabilized with respect to a planar local excited state. Since the highly twisted form is energetically destabilized in the ground state, TICT formation brings the excited and ground states closer, permitting more rapid internal conversion (see Scheme 2). The concept of intramolecular electron transfer as an alternative mode of action for ultraviolet stabilizers has been suggested,[26] and TICT states have been observed in ether derivatives of hydroxyphenyltriazine UVAs.[26,27] However, for the triazine ethers, TICT states are longer lived than the locally excited states, allowing more time for competitive photoreaction. As a result, the ethers serve as poor UVAs. In benzotriazole species, the elements of donor (phenol)[28] and acceptor (triazole)[29] are present, and so the possibility also exists for TICT states in these species.[5] Therefore, we explored the effects of

[†] Columbia University.
[‡] Ciba Specialty Chemicals.

10.1021/jp021000j CCC: $22.00
Published on Web 07/31/2002

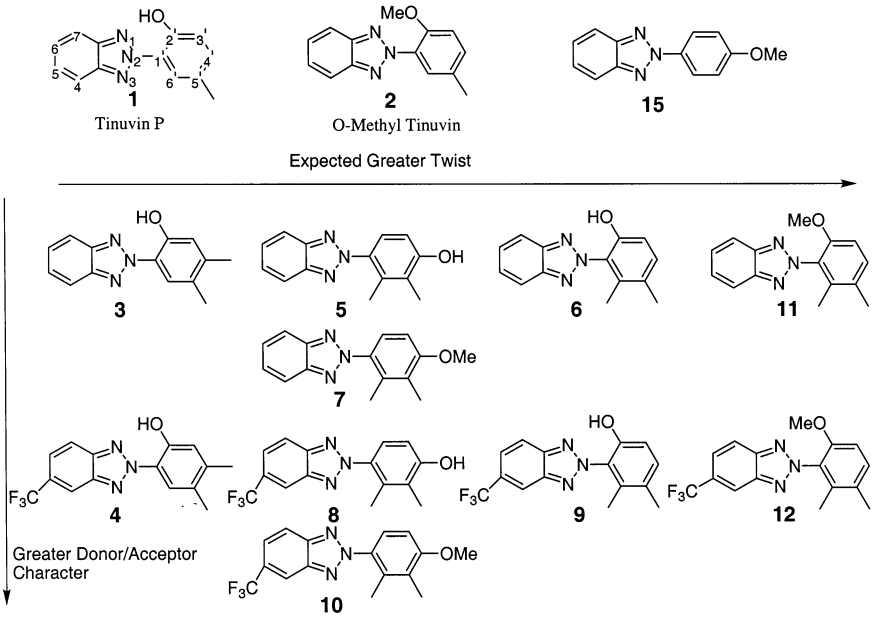

Figure 1. Arylbenzotriazoles studied. Ordered on the basis of the expected degree of twist along triazole C−N bond and donor/acceptor character.

SCHEME 1: Paradigm for ESIPT Deactivation[a]

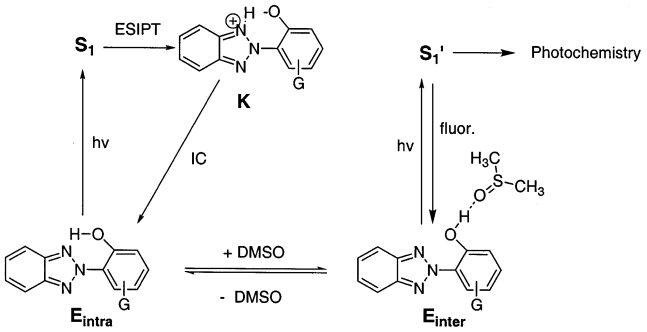

[a] G denotes different functional groups substituted on the phenyl ring.

SCHEME 2: Paradigm for TICT Deactivation[a]

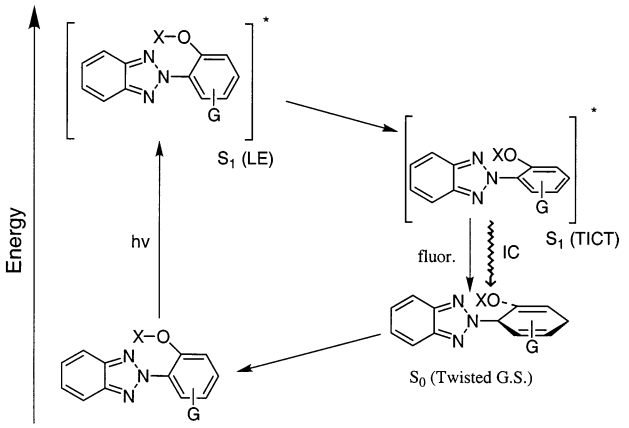

[a] G represents functional groups attached to the aryl ring (X = H or Me).

structural modification on the photophysics of various 2-arylbenzotriazoles.

In this paper we report the photophysical properties of a series of 2-arylbenzotriazole compounds illustrated in Figure 1. The compounds are ordered with respect to the expected degree of twist and the degree of donor/acceptor character. The specific features installed in these compounds in order to enhance a potential TICT effect are the 6′-methyl group which provides additional propensity to twist in these compounds,[11,30] and the addition of the trifluoromethyl group to the triazole ring, which is expected to enhance donor/acceptor character.[31] Furthermore, the substitution patterns were varied to investigate the influence of the degree of twist. The results indicate that a charge transfer mechanism is involved in singlet deactivation of compounds that possess both a large degree of twist and donor/acceptor character. The mechanism for TICT deactivation is outlined in Scheme 2. The locally excited (Franck−Condon) state rapidly twists and undergoes intramolecular electron transfer to form the TICT state. The TICT state deactivates by internal conversion through either a close approach or a conical intersection with the ground state.[32]

We have found that twisted hydroxybenzotriazoles such as **6** undergo dynamic fluorescence quenching in the presence of weak bases such as dimethyl sulfoxide (DMSO). These results are discussed in the context of deactivation via either partial or complete intermolecular proton transfer to solvent (PTTS) from the TICT state (see Scheme 3).[33−37] In this process, either partial or full proton transfer from the benzotriazole to DMSO results in deactivation of the excited state. Although intermolecular proton transfer has been observed previously with Tinuvin P,[20] in this case, no significant fluorescence deactivation was observed. Although the intermolecular proton transfer can be reversible in the case of Tinuvin P, the long lifetime of the phenolate anion (80 μs in argon purged DMSO) allows for side reactions such as oxidation of the phenolate anion.[20] In the case of the twisted hydroxybenzotriazole, **6**, initial photostability results show that this compound undergoes reduced photodegradation in the presence of DMSO. The enhanced photostability of **6** in DMSO supports the possibility of excited state deactivation through an aborted proton transfer, although other possibilities cannot be ruled out.

Our results suggest that although donor/acceptor character is significant for TICT deactivation, the degree of twist is the more important parameter. The compounds in this study provide a clear example of a TICT excited singlet state deactivation mechanism for the benzotriazole UVAs and provide a potential new deactivation manifold for exploration toward the preparation of better UVAs.

SCHEME 3: Paradigm for Deactivation through Intermolecular Proton Transfer[a]

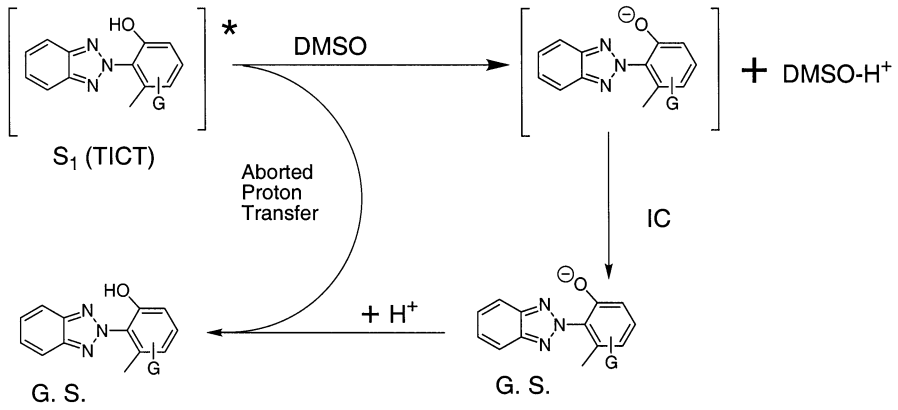

[a] The TICT excited state deactivates to the ground state (G.S.) through either a partial (aborted) or complete proton transfer to DMSO.

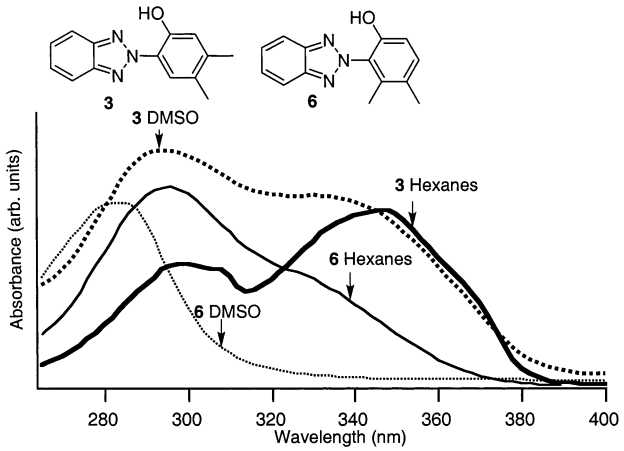

Figure 2. UV-absorption spectra of compounds **6** and **3** in hexanes and DMSO.

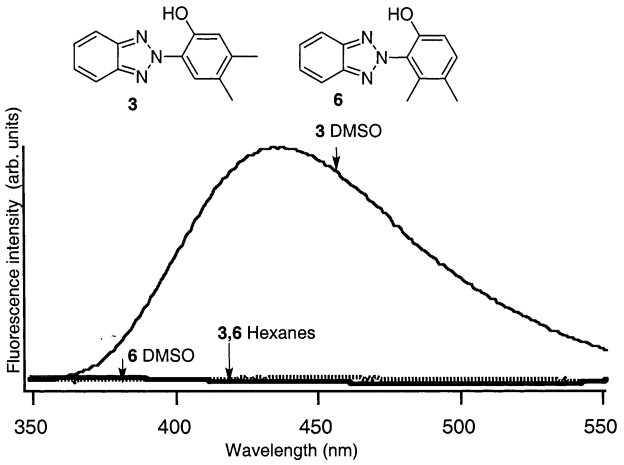

Figure 3. Steady state emission of compounds **6** and **3** in hexanes and DMSO. Excitation at 290 nm.

Results

Steady State UV and Fluorescence Spectra. UV−vis absorption and fluorescence spectra are illustrated in Figures 2 and 3 for compounds **6** and **3**. The photophysics of compound **3** is completely analogous to Tinuvin P (**1**).[17] The observation of a long wavelength UV−vis absorption in hexanes at ∼345 nm is characteristic of an intramolecular hydrogen bond.[38] Due to the intramolecular hydrogen bond, **3** deactivates via the standard ESIPT mechanism.[17] Hence, it is essentially nonfluorescent. In DMSO, the UV−vis spectra of **3** shows a decrease

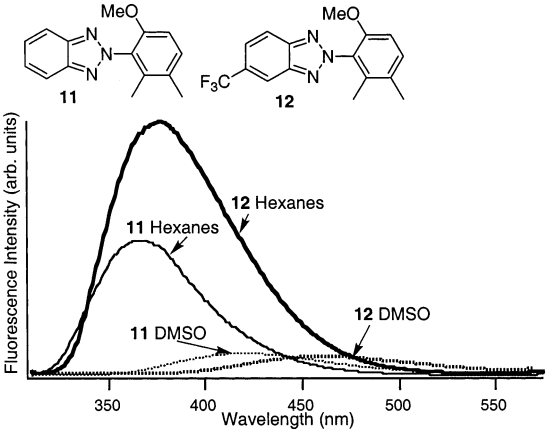

Figure 4. Steady state emission of compounds **11** and **12** in hexanes and DMSO. Excitation at 290 nm.

in the amount of absorption in the ∼345 nm band and a dramatic increase in the amount of fluorescence. This result is consistent with the current mechanistic paradigm for singlet excited state deactivation of benzotriazole UVAs such as Tinuvin P (**1**, Figure 1). The decrease in the long wavelength absorption is interpreted as a breakage of the intramolecular hydrogen bond. Without the intramolecular hydrogen bond, the ESIPT deactivation mechanism can no longer operate, resulting in fluorescence.[38] Compound **6**, an isomer of **3**, with the methyl group at the 6′ position rather than the 4′ position, has an intramolecular hydrogen bond in hexanes and, as expected, shows no fluorescence. However, in DMSO, the ∼345 nm band is absent, showing that the intramolecular hydrogen bond is completely broken; nevertheless, the compound still shows almost no fluorescence ($\Phi_f \sim 10^{-4}$). This result disagrees with the standard paradigm for benzotriazole UVAs, which predicts that the loss of the hydrogen bond will lead to the onset of significant fluorescence.[10,20]

The methyl ethers **11** and **12**, neither of which possess an intramolecular hydrogen bond, both display reduced fluorescence in DMSO as compared to hexanes (see Figure 4). In addition, the fluorescence is strongly red shifted. The quenching of fluorescence is more dramatic for **12** than for **11**.

Fluorescence quantum yields are presented in Table 1. The quantum yields are reported relative to *o*-methyl Tinuvin **2** in DMSO ($\Phi_f = 0.135$).[39] Comparison of compounds **5** and **8** indicates that in DMSO the addition of a trifluoromethyl group to the triazole ring decreases Φ_f by an order of magnitude. On the other hand, in hexanes, the electron withdrawing group has no effect on Φ_f. Exceptionally low quantum yields of fluores-

TABLE 1: Quantum Yields of Fluorescence in Hexanes and DMSO

compound	Φ_f hexanes	Φ_f DMSO
4	$<10^{-5}$	$5 \times 10^{-4} \pm 4 \times 10^{-5}$
9	$1.2 \times 10^{-3} \pm 2 \times 10^{-4}$	$<10^{-5}$
3	$<10^{-5}$	$6 \times 10^{-3} \pm 5 \times 10^{-4}$
5	0.27 ± 0.03	$(0.02 \pm 3) \times 10^{-3}$
8	0.27 ± 0.01	$(0.001 \pm 4) \times 10^{-4}$
6	$<10^{-5}$	$2 \times 10^{-4} \pm 1 \times 10^{-4}$
7	0.27 ± 0.05	0.14 ± 0.03
10	0.31 ± 0.04	0.07 ± 0.02
11	0.08 ± 0.04	$(0.02 \pm 3) \times 10^{-3}$
12	0.10 ± 0.05	$(0.01 \pm 3) \times 10^{-3}$

cence are found in DMSO for the hydroxy compounds with both 2′ and 6′ groups on the aryl ring (compare compounds **6** and **9** with compound **3**). In the case of isomers **3** and **6** in DMSO, moving the methyl group from the 4′ to the 6′ position results in a 30-fold decrease in Φ_f . Addition of the trifluoromethyl group (**9**) drops Φ_f below our detection limits in DMSO ($\Phi_f < 10^{-5}$). The less twisted isomers **3** and **4** exhibit weak fluorescence in DMSO ($\Phi_f \sim 10^{-2}-10^{-3}$).

Fluorescence Lifetimes. *Phenols.* The fluorescence lifetimes were measured by single photon counting (SPC) for **5**, **6**, and **8** under varying conditions in order to assess the relative importance of polarity and basicity on the fluorescence decay. The pulse width of the lamp was ca. 1.5 ns. All compounds were excited at 290 nm. Emission was observed for **5** at 433 nm, for **6** at 420 nm, and for **8** at 440 nm. Lifetimes were calculated from the decay traces using a reconvolution analysis with the lamp profile, and the data were fit to a monoexponential. This analysis generated fits with reasonable χ^2 for the longer lifetime measurements. For compounds with shorter lifetimes (<0.8 ns) the values quoted are estimates based on reconvolution analysis. The measurements do indicate clearly and reproducibly that the lifetime has decreased significantly; however, the accuracy in the measured lifetimes is limited by the resolution of our instrument. We estimate the uncertainty in the short lifetime measurements to be approximately ±0.2 ns.

Table 3 illustrates the special quenching effect of DMSO on the fluorescence of these hydroxy compounds. In each case, DMSO, whose polarity is similar to acetonitrile,[40,41] significantly reduces both the fluorescence lifetime and the steady state emission. The reduction in lifetime tracks roughly with the reduction in steady state fluorescence, indicating a predominantly dynamic quenching process with DMSO. The effectiveness of DMSO quenching increases with the number of ortho substituents and also when an electron-withdrawing group is present on the triazole ring (compare **6** and **8** with **5**). Compound **3** shows identical behavior in DMSO and acetonitrile (vide infra).

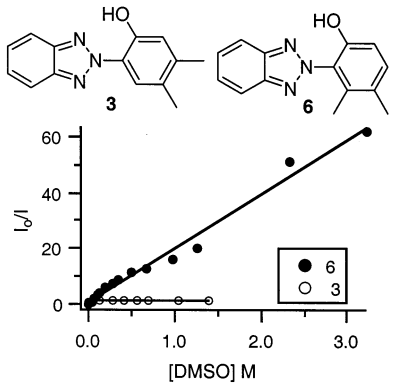

Figure 5. Stern−Volmer plot of DMSO fluorescence quenching of **3** and **6** in acetonitrile. Excitation at 290 nm.

*DMSO Quenching of the Fluorescence of **6**. Stern−Volmer Analysis.* The steady state fluorescence of **3** and **6** was measured in acetonitrile as a function of increasing DMSO concentration. The Stern−Volmer plot of the results are presented in Figure 5. In the case of compound **3**, the steady state fluorescence changes only very slightly upon addition of DMSO. Compound **6**, on the other hand, showed a dramatic decrease in fluorescence emission upon addition of DMSO. The absorption spectra of **6** is not affected by added DMSO. The emission maximum is slightly red shifted on addition of DMSO. The slope ($k_q\tau_F$) of the Stern−Volmer curve for **6** is 19.4 ± 0.7 M^{-1} in acetonitrile. Using the fluorescence lifetime (τ_F) as measured using single photon counting, the dynamic quenching constant (k_q) is calculated to be $2 \times 10^{10} \pm 1 \times 10^9$ M^{-1} s^{-1}.

For compound **3** the UV−vis spectrum changes with addition of DMSO, resulting in a decrease of the amount of long wavelength (~340 nm) absorption. At 1.4 M DMSO, the

TABLE 2: Emission and Absorption Maxima for Compounds Studied in Different Solvents

	hexanes		cyclohexane		ether		THF		DMSO		methanol	
comp.	abs	em	abs	em	abs	em	abs	em	abs	em	abs	em
4	300, 358	x							291	464		
9	297	373							284	x		
3	300, 346	376							294	437		
5	292	377							288	435		
8	298	386							296	457		
6	296, 326	376							284	446		
7	294	381	294	384	290	390	292	397	290	419	288	421
10	300	387	300	383	298	407	298	416	294	441	296	441
11	286	368	286	367	286	380	282	385	282	415	280	437
12	282	378	284	378	282	404	282	423	282	460	280	464
15			320	378	318	380	320	387	320	402	318	401

TABLE 3: Steady State Fluorescence Emission Intensities and Fluorescence Lifetimes for 6, 8, and 5 in Acetonitrile with Varying Amounts of DMSO[a]

	6		**8**		**5**	
conditions	$I_f$rel	τ_f (ns)	$I_f$rel	τ_f (ns)	$I_f$rel	τ_f (ns)
MeCN	2.3	0.8 ± 0.1	4.5 ± 0.5	0.8 ± 0.1	5.5 ± 0.5	0.8 ± 0.1
2.5% DMSO	1	0.3 ± 0.2	1	0.4 ± 0.2	X	X
100% DMSO	X	X	X	X	1	0.2 ± 0.2

[a] X means that these measurements were not performed.

TABLE 4: Comparison of Steady State Fluorescence Quantum Yields versus Lifetimes for 12, 7, 10, and 11[a]

compound		hexanes	DMSO	MeCN
7	τ_f (ns)	1.7 ± 0.1	1.0 ± 0.1	1.0 ± 0.1
	Φ_f	0.27 ± 0.05	0.14 ± 0.03	0.15 ± 0.01
	Φ_f/τ_f ($s^{-1} \times 10^8$)	1.6	1.4	1.5
10	τ_f (ns)	1.8 ± 0.1	1.0 ± 0.1	X
	Φ_f	0.31 ± 0.04	0.07 ± 0.02	X
	Φ_f/τ_f ($s^{-1} \times 10^8$)	1.7	0.7	X
11	τ_f (ns)	1.1 ± 0.1	0.8 ± 0.1	X
	Φ_f	0.08 ± 0.04	$(0.02 \pm 3) \times 10^{-3}$	X
	Φ_f/τ_f ($s^{-1} \times 10^8$)	0.7	0.25	X
12	τ_f (ns)	1.7 ± 0.1	1.3 ± 0.1	1.0 ± 0.1
	Φ_f	0.10 ± 0.05	$(0.01 \pm 3) \times 10^{-3}$	$(0.01 \pm 3) \times 10^{-3}$
	Φ_f/τ_f ($s^{-1} \times 10^8$)	0.6	0.08	0.1

[a] X means experiment was not performed.

TABLE 5: Results from Lippert−Mataga Plots

compound	slope (cm^{-1})	intercept (cm^{-1})	$\Delta\mu$ (D)	μ_g (D)[a]	μ_e (D)
12	$18169 \pm 2{,}400$	8418 ± 528	17.3 ± 1.1	4.3	21.6 ± 1.1
11	15868 ± 4100	7027 ± 893	16.2 ± 2.1	1.6	17.8 ± 2.1
10	13812 ± 1700	7038 ± 1373	15.1 ± 0.9	3.8	18.9 ± 0.9
7	9802 ± 2300	7649 ± 503	12.7 ± 1.5	1.3	14.0 ± 1.5
15	5768 ± 1600	4560 ± 345	9.7 ± 1.4	1.4	11.1 ± 1.4
DMABN (TICT)					13.7[b,45]
DMABN (LE)					10.1[b,45]

[a] Dipole moments calculated using Spartan−HF/6-31G(d) scaled by 0.87. [b] Determined by same solvatochromic method.

absorption at 340 nm is 75% of its value in neat acetonitrile (see Supporting Information for details). The change in the UV−vis spectrum is indicative of an increase in the amount of open form. Thus the ESIPT paradigm suggests an increase in the amount of fluorescence upon addition of DMSO. Although the increase in the amount of open form could obscure DMSO induced quenching for compound **3**, the open form fluorescence would only have a minor effect on the Stern−Volmer plot. Taking into account this interference, we estimate that the maximal Stern−Volmer constant ($k_q\tau_F$) for **3** would be ca. 0.7 M^{-1}.

Methyl Ethers. SPC was used to measure fluorescence lifetimes for the methyl ethers (see above for experimental details). The SPC data for the methyl ethers were fit to monoexponential decays, with reasonable χ^2. The lifetimes (τ_F) of the methyl ethers **7**, **10**, **11**, and **12** were compared with the steady state emission intensities I_f as a function of solvent (see Table 4). Although a dramatic decrease in I_f is observed on switching to more polar solvents (DMSO, acetonitrile), the lifetimes vary only slightly as a function of solvent. The difference in the ratio of the steady state emission intensity versus fluorescence lifetime increases as the number of ortho substituents is increased from one to two, and upon introduction of an electron-withdrawing substituent to the triazole ring. In the case of **12**, the steady state emission intensity changes by an order of magnitude going from hexanes to DMSO; however, the lifetime varies only slightly for this dramatic polarity change.

Lippert−Mataga Plots. Lippert−Mataga analysis was performed on the methyl ether compounds in order to estimate the magnitude of the excited state dipole moment in these compounds. The energy difference of the fluorescence maximum relative to the absorption maximum as a function of the solvent orientation parameter (Δf) has been used as a measure of the change in dipole moment between the fluorescing excited state and the ground state.[42,43] Equation 1, from Lippert−Mataga theory, shows that the energy difference ($\nu_{abs} - \nu_{flu}$ in cm^{-1}) is proportional to the orientation parameter (Δf).[43] The Onsager radius[44] (**a**) is estimated from computer models (using Chem 3D) to be 5.5 Å, h is Planck's constant, and c is the speed of light:

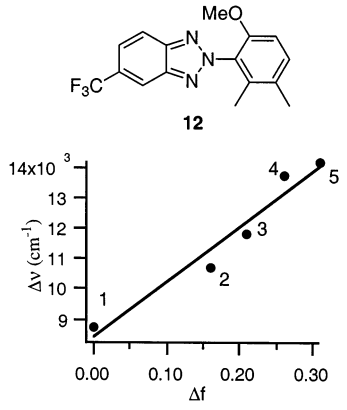

Figure 6. Lippert−Mataga plot for **12** with Δf = orientation parameter.[42] Solvents: cyclohexane (1), ether (2), tetrahydrofuran (3), dimethyl sulfoxide (4), methanol (5).

$$\bar{\nu}_{abs} - \bar{\nu}_{flu} = [2(\mu_e - \mu_g)2/hc\mathbf{a}^3]\Delta f + \text{const} \qquad (1)$$

Figure 6 plots $\nu_{abs} - \nu_{flu}$ in wavenumbers for compound **12**. The slope of this line can be used to calculate the change in dipole moment on excitation of **12** using the Lippert−Mataga theory. These values are presented for the methyl ethers **7**, **10**, **11**, **12**, and **15** in Table 5. These values can be compared with dimethylaminobenzonitrile (DMABN), an exemplar TICT compound, which is also listed in Table 5.[45] Notice that for **10**, **11**, and **12**, the change in dipole on excitation is much larger than the reported value for DMABN's TICT state as determined by the same method.[45] The value calculated for the nontwisted compound **15**, is similar to that of the locally excited FC state of DMABN. Unlike DMABN, in the case of all the compounds in this study, only one fluorescence was observed.

Furans. The furan compounds **13** and **14** possess both planar and nonplanar conformations (from UV−vis spectroscopy). DMSO appears to shift the equilibrium more toward the nonplanar state (see Figure 7). Interestingly, these results indicate

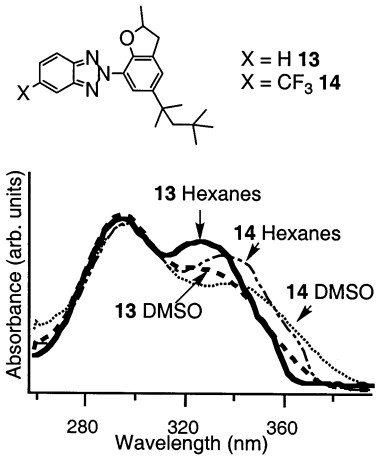

Figure 7. UV−vis absorption spectra of furans **13** and **14**.

that in the absence of steric repulsion, these compounds favor a planar structure even without the aid of an intramolecular hydrogen bond. The shift to more open form in DMSO suggests the possibility of charge transfer in the ground state.

Discussion

The incorporation of a methyl group in the 6′ position of the 2-(2′-hydroxyphenyl)benzotriazole structure radically alters the photophysics of this class of UVAs by enhancing a new fluorescence deactivation mechanism which competes with or replaces the standard ESIPT mechanism. Of the several possible mechanisms of deactivation, the effect is attributed to a twisted intramolecular charge transfer (TICT) process as indicated by several pieces of evidence: (1) more efficient fluorescence deactivation in polar solvents, (2) more efficient fluorescence deactivation upon introduction of donor groups on the phenyl ring and acceptor groups on the benzotriazole ring, (3) more efficient fluorescence deactivation upon introduction of 6′ substituents in the phenyl ring (consistent with the rule of minimum overlap in TICT states), and (4) large Stokes shifts in fluorescence on changing solvent from hexanes to DMSO ($\sim$4700 cm^{-1} for **12**) corresponding to a large change in excited state dipole of (17.3 $\pm$ 1.1 D).[22] Some other possibilities for deactivation have been ruled out. Minor changes in absorption spectra going from nonpolar to polar solvents and the observation of dynamic quenching effects rule out ground state complexation. Energy transfer to solvent is not possible with either DMSO or acetonitrile. ESIPT mechanisms in DMSO are ruled out by either structure or by UV−vis data (no closed forms in DMSO for 6′-methyl compounds). Phosphorescence measurements at 77 K of **6** and **11** (not shown) showed similar or smaller emission intensities compared to Tin P, indicating that intersystem crossing is no more important in the 6′-methyl compounds than in Tin P.

In the case of the methyl ethers (compounds **7**, **10**, **11**, and **12**), polarity is the most important solvent parameter in the new deactivation scheme, since both the ESIPT mechanism and the intermolecular proton transfer are not possible. For the hydroxy compounds (compounds **4**, **5**, **6**, and **8**), the situation is more complicated. Although polarity is important, solvent basicity and hydrogen bond acceptor strength are also important. The hydroxy compounds have the possibility of both an intramolecular and intermolecular proton transfer deactivation mechanism (Scheme 3), each of which is influenced by solvent.

With regard to the substrate, the two issues of donor/acceptor effects and twist appear important in both the qualitative and quantitative aspects of fluorescence deactivation.

SCHEME 4: Paradigm for Photophysics of Methyl Ethers

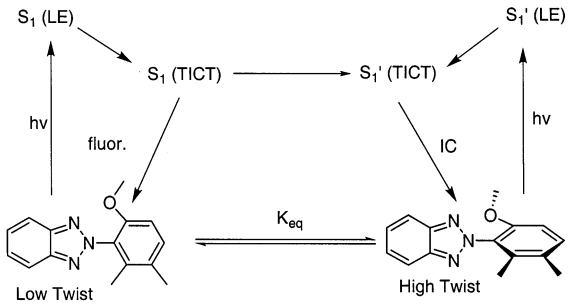

Our measurements of the excited state dipole moments in the methyl ethers (see Table 5) using the Lippert−Mataga theory support the hypothesis of a TICT excited state. The compounds containing both 2′ and 6′ ortho substituents (**11** and **12**) have the largest changes in dipole moment upon excitation, 16.2 and 17.3 D, respectively, leading to extremely large excited state dipole moments. Compound **10**, which has a sizable ground-state dipole due to the presence of a trifluoromethyl group, also exhibits a large excited state dipole moment that is comparable in size to compound **11**. Compound **7**, however, has a lower dipole moment, due to the fact that it has only one ortho substituent, and does not have an electron withdrawing trifluoromethyl group on its triazole ring. The ordering of excited state dipole moments is consistent with the ordering of polar solvent assisted excited singlet state deactivation (see Table 1), and is in agreement with the principles for stabilization of TICT states.[23]

Comparison of the fluorescence quantum yields and the lifetimes for **10**, **11**, and **12** (see Table 4) indicate that the variations in Φ_f are not parallel with the variations of τ_f on going from a nonpolar to a polar solvent. The results suggest that a large degree of the fluorescence is quenched by a process occurring faster than the response time of our instrument. For **7**, which has both a lower degree of twist and donor/acceptor character, Φ_f/τ_f is constant for the different solvents.

We propose that compounds **10**, **11**, and **12** possess two conformational states, a faster deactivating state (shorter than our instrument's response) and a longer lived fluorescent state ($\tau_f \sim 1-2$ ns). Similar results were observed for the TICT states of the triazine ethers.[27] However, in that case, the shorter lifetime component corresponded to the locally excited state, whereas the longer lifetime component was assigned to the TICT state. We suggest that in our system, both states are TICT states. It is likely that the two states are conformers with a varying degree of twist around the benzotriazole−aryl C−N bond and/or difference in conformation of the methoxy group (see Scheme 4). The strong Stokes shift in the steady state fluorescence for compounds **7**, **10**, **11**, and **12** and the large excited state dipole moments support the TICT nature of the longer lived excited state. The correlation of the magnitude of deactivation with greater twist and greater donor−acceptor character supports the hypothesis that the shorter lived excited state is also TICT in nature.

We propose that the behavior of Φ_f and τ_f can be explained based upon Scheme 4. In this scheme, we postulate two ground state conformations. Upon excitation of either of these conformers, the initial locally excited states S_1(LE) and S_1'(LE) quickly relax to the TICT states S_1(TICT) and S_1'(TICT). The state S_1(TICT) fluoresces. The fluorescence from S_1(TICT) was used to measure the excited state dipole moment (Table 5). The presence of S_1'(TICT) is inferred from a discrepancy between

the steady state and fluorescence lifetime measurements for compounds **10**, **11**, and **12** (see Table 4). As structural features are added, which push the equilibrium of the ground state to the postulated high twist form, the decrease in Φ_f becomes larger than the decrease in τ_f. This result supports the hypothesis that the rapidly deactivating state is, in fact, also a TICT state. In all cases the dynamic component of fluorescence quenching (i.e., the change in lifetime as a function of solvent polarity) results from the deactivation pathway in which the S_1 conformer converts on the excited state surface to the S_1' conformer followed by internal conversion (see Scheme 4).

In the case of compound **12**, the conformation of the methoxy group (methyl syn or anti to the benzotriazole ring) may be the critical parameter determining the conversion between the two states (see Scheme 4). When the methyl group is pointing away from the triazole ring, a more planar structure may be favored, taking advantage of energetic stabilization via conjugation of the benzotriazole ring with the phenyl ring. When the methyl group is pointing toward the benzotriazole ring, the twisted state may be favored for both steric reasons as well as electronics, if there is some charge transfer character in the ground state. This hypothesis is supported by data for the furan compounds, **13** and **14**, which show a long wavelength band in their UV absorption spectra consistent with a significant population of a planar conformer (see Figure 7). As in the case of Tinuvin P, the presence of the long wavelength band is indicative of a planar conformer. In DMSO, the long wavelength band is reduced (see Figure 7), indicating a decrease in the amount of the planar conformer. The ability of the polar solvent to increase the amount of nonplanar conformer is consistent with the presence of some charge transfer character in the ground state of this conformer.

Compound **12** has both a 2′-methoxy and a 6′-methyl which favor the high twist side of the equilibrium in the ground state. The presence of the trifluoromethyl group in the benzotriazole ring would significantly stabilize charge transfer, and also favor the higher twist side of the equilibrium. In the case of **7**, which has only one ortho group and no electron withdrawing group on the triazole ring, Φ_f and τ_f both decrease by a factor of 2 going from hexanes to DMSO. This fact can be explained by the lower degree of twist, resulting in a lower equilibrium amount of high twist compound. Furthermore, the absence of the trifluoromethyl group in the benzotriazole ring would reduce the amount of stabilization of the TICT state, decreasing its rate of deactivation. Compound **10**, which has a trifluoromethyl group in the benzotriazole ring in addition to the 6′-methyl group, shows a 4-fold decrease in Φ_f on switching from hexanes to DMSO, yet only a 2-fold decrease in τ_f . Compound **11**, which has two ortho groups on the phenyl ring, shows a 5-fold decrease in Φ_f on switching from hexanes to DMSO, yet only a 1.5-fold decrease in τ_f.

Upon analysis of the quantum yields of fluorescence in Table 1, we can conclude that ortho substitution is more important than donor/acceptor character for the TICT deactivation mechanism in methyl ethers. Notice that for the compounds **10** and **7**, each with only one ortho group, the fluorescence deactivation is approximately the same in hexanes. In DMSO, the trifluoromethyl group in the benzotriazole ring reduces Φ_f for **10** only by a factor of 2. In combination with a 2′-methoxy group, the 6′-methyl effect is much more dramatic. Comparing compounds **7** and **11**, we see a drop in Φ_f in both hexanes and DMSO on moving the methoxy group from the 4′ to the 2′ position ($\sim$3.5$\times$ and 7$\times$ reduction in Φ_f, respectively). Compounds **10** and **12** mirror this trend (3$\times$ and 7$\times$ reduction in Φ_f). The enhanced twist, therefore, appears to be the most important factor in the TICT deactivation pathway. The donor/acceptor character, nevertheless, is also important, and the largest deactivation rates are observed for compound **12**, which incorporates both the twist (2′ + 6′ substitution) and charge transfer (trifluoromethyl group in triazole ring) features.

Intermolecular and intramolecular hydrogen bonding in the twisted state offer additional pathways for deactivation for the phenolic benzotriazoles. In the intermolecular process, the excited state can relax to a conical intersection[32,36,46,47] through partial or complete proton transfer to solvent,[34] resulting in ultrafast return to the ground state (see Scheme 3). With 2-(2′-hydroxyphenyl)benzotriazoles, such as Tinuvin P, it has been shown by laser flash photolysis that the deprotonation from the excited state occurs in basic solvents such as DMSO.[20] However for Tinuvin P, DMSO serves to destabilize the planarity of the molecule, resulting in an enhancement of fluorescence through the loss of the competing ESIPT mechanism. In compounds in which a 6′-methyl group is installed, e.g., **6** or **9**, although DMSO disrupts the intramolecular hydrogen bond, virtually no fluorescence is observed ($\Phi_f \sim 10^{-4}-10^{-5}$). The effect is peculiar to the 6′-methyl compounds (compare compounds **3** and **6** in Table 1 and see Figure 3), suggesting that a twist between the benzotriazole and phenyl rings is essential for increasing the efficiency of this mechanism of deactivation.

In compounds with a lower degree of twist (compare **5** and **8**), the introduction of an electron withdrawing group into the BZT-ring and a polar environment triggers the TICT deactivation mechanism.

By studying the fluorescence of compound **6** as a function of DMSO concentration and comparing this with lifetime measurements, it is seen from the Stern−Volmer plot (Figure 5) that dynamic quenching occurs with $k_q = 2 \times 10^{10}$ M^{-1} s^{-1}. Note that for the isomer **3**, which does not possess a 6′-methyl (i.e., similar to Tinuvin P), no significant DMSO induced deactivation is observed. These data are all consistent with fluorescence deactivation through either partial or complete excited state proton transfer to DMSO (see Scheme 3). Partial proton transfer from the substrate to DMSO could lead the substrate toward a conical intersection and hence permit fast deactivation.[36,48] Although intermolecular proton transfer could potentially reduce photostability by producing a reactive phenolate anion,[20] initial stability studies indicate that **6** is actually photostabilized in the presence of DMSO.[49] The enhanced photostability of **6** in DMSO supports the possibility of excited state deactivation through an aborted proton transfer rather than full PTTS.

The results for the methyl ethers corroborate these findings. In the methyl ether series, DMSO and acetonitrile behave similarly in their effects on fluorescence, as would be expected considering their identical polarities (as defined by Kosower *Z* values 71.1 and 71.3, respectively).[40,41]

Conclusion

The 2-(hydroxy or methoxy-6′-methylaryl)benzotriazoles present a new class of compounds exhibiting TICT excited states. The twisted-hydroxy benzotriazoles have an interesting photochemical trigger for excited state deactivation via intermolecular proton transfer to basic solvents. The methoxy compounds have an interesting equilibrium between a roughly planar and a highly twisted form, each of which has unique photophysical properties. The highly twisted form can deactivate through charge transfer which accelerates the rate of internal conversion. The planar form is capable in the excited state of

either fluorescence or conversion to the more highly twisted form followed by deactivation. Donor/acceptor character in the phenyl and benzotriazole portions is important to the rates of deactivation. However, the steric effects which generate a twist in the ground and excited states are essential for increasing the efficiency of this mechanism of deactivation.

The complex photophysics and photochemistry of these compounds will, no doubt, provide material for several further studies and applications, and prove to be an interesting area for future UVA research. A thorough understanding of the interplay between ESIPT, excited state intermolecular proton transfer, and intramolecular electron transfer mechanisms (TICT) will allow for the tailoring of compounds with very useful properties as UVAs and potentially in other applications. For example, the ability of the (hydroxyaryl)benzotriazoles to switch between fluorescent and nonfluorescent states as a function of environment could be exploited in applications such as molecular probes and switches.

Experimental Section

Materials and Solvents. DMSO, cyclohexane, and hexanes were of spectrophotometric grade from Aldrich. THF (HPLC grade) was from ACROS. Acetonitrile and methanol were Optima grade from Fisher. Diethyl ether was from Mallinckrodt. Solvents were tested for background absorption and emission prior to use.

Measurements. UV−vis absorption spectra were recorded on an HP8452A UV spectrometer. Fluorescence spectra were measured with a Spex FluoroMax-2 spectrometer using a 1 cm × 1 cm quartz cell and concentrations such that the optical density was approximately 0.1 at the excitation wavelength (290 nm). Time-resolved fluorescence lifetimes were performed by single photon counting on a OB900 fluorometer (Edinburgh Analytical Instruments).

Synthetic Procedures. *General Details.* Unless otherwise specified, all reagents were purchased from commercial suppliers and used without further purification. ^{1}H NMR (300.08 and 499.84 MHz, respectively) spectra were obtained on a Varian Gemini 300 MHz w/ASM-100 or a Unity 500 MHz spectrometer. All ^{1}H chemical shifts are reported in ppm relative to tetramethylsilane, where a positive sign is downfield from the standard. ^{19}F NMR spectra (282.33 MHz) were obtained on a Varian Gemini 300 MHz w/ ASM-100. ^{19}F NMR chemical shifts are reported in ppm relative to CF_3COOH at −70.0 ppm. Mass spectra were obtained on a Fisons VG Platform II in APcI mode using a Hewlett-Packard LC II for sample delivery. Elemental analyses were obtained from Robertson Microlit Laboratories, Madison, NJ. Merck silica gel 60 (200−400 mesh) was used for column chromatography. Merck precoated (0.25 mm) silica gel F-254 plates were used for TLC. Solvents were dried prior to use when necessary with appropriate drying agents. Reactions were carried out in dried apparatus under a dry inert atmosphere of nitrogen.

General synthetic procedures for benzotriazole ring construction are found in U.S. Patents 5,977,219 and 6,166,218. Compounds for photophysical studies were purified sequentially by chromatography (silica gel) and sublimation, except **14**, which was chromatographed twice on silica gel and sublimed.

*2-[2-Methyl-5-(1,1,3,3-tetramethylbutyl)-2,3-dihydrobenzofuran-7-yl]-5-(trifluoromethyl)-2H-benzotriazole (**14**).* A mixture of 5-(trifluoromethyl)-2-(2-hydroxy-5-*tert*-octylphenyl)-2*H*-benzotriazole (13.01 g, 0.033 mol), potassium hydroxide (2.37 g, 0.036 mol), and ethanol (60 mL) was stirred at ambient temperature for 2 h. To the reaction mixture, allyl bromide (4.84 g, 0.039 mol) and potassium iodide (0.34 g, 0.002 mol) were added portion wise, after which the reaction mixture was heated to 85 °C. After holding at 85 °C for 4.5 h, the solvent was removed by distillation and replaced with 100 mL of heptane. The mixture was washed three times with 40 mL of water. The solvent was then removed by distillation to yield 14.2 g (99%) of the corresponding O-allyl ether as an off-white solid. ^{1}H NMR ($CDCl_3$): δ 8.35 (s, 1H), 8.20−8.12 (d, 1H), 7.67−7.61 (m, 2H), 7.54−7.49 (dd, 1H), 7.11−7.06 (d, 1H), 6.00−5.86 (m, 1H), 5.34−5.16 (m, 2H), 4.65−4.60 (d, 2H), 1.77 (s, 1H), 1.41 (s, 6H), 0.78 (s, 9H).

The O-allyl compound (14.2 g) as prepared above was added to a round-bottom flask, heated to 190−195 °C, and held at that temperature for 5 h. The residue was purified by flash column chromatography with silica gel (ethyl acetate/heptane gradient) to give 12.2 g (86%) of the C− allyl substituted benzotriazole as a yellow oil. MS *m*/*z* 432 (M+H); ^{1}H NMR ($CDCl_3$): δ 11.17 (s, 1H), 8.35−8.29 (m, 2H), 8.12−8.05 (d, 1H), 7.72−7.66 (dd, 1H), 7.34−7.29 (d, 1H), 6.18−6.02 (m, 1H), 5.20−5.06 (m, 2H), 3.64−3.53 (d, 2H), 1.81 (s, 2H), 1.46 (s, 6H), 0.78 (s, 9H).

A mixture of 5-(trifluoromethyl)-2-(2-hydroxy-3-allyl-5-*tert*-octylphenyl)-2*H*-benzotriazole (12.16 g, 0.028 mol), methanesulfonic acid (3.34 g, 0.034 mol), and chlorobenzene (50 mL) was heated to 140 °C and held there for 3 h. After removal of solvent, the brown oil was chromatographed twice on silica gel (19:1 hexane/ethyl acetate) to yield 1.21 g (10%) as a yellow viscous resin. ^{1}H NMR ($CDCl_3$): δ 8.36 (s, 1H), 8.12 (d, 1H), 7.87 (s, 1H), 7.60 (d, 1H), 7.35 (s, 1H), 5.21 (m, 1H), 3.47 (dd, 1H), 2.94 (dd, 1H), 1.79 (s, 2H), 1.57 (d, 3H), 1.44 (s, 6H), 0.8 (s, 9H); MS *m*/*z* 432 (M+H). Anal. Calcd for $C_{24}H_{28}F_3N_3O$: C, 66.81; H, 6.54; N, 9.74. Found: C, 66.10; H, 6.25; N, 9.76.

*2-[2-Methyl-5-(1,1,3,3-tetramethylbutyl)-2,3-dihydrobenzofuran-7-yl]-2H-benzotriazole (**13**).* The synthesis of this compound followed the same synthetic conditions used for compound **14**. A white solid (0.61 g, 5%) was obtained with a melting point of 128−128.5 °C. ^{1}H NMR ($CDCl_3$): δ 8.00 (m, 2H), 7.85 (s, 1H), 7.42 (m, 2H), 7.30 (s, 1H), 5.22 (m, 1H), 3.43 (dd, 1H), 2.93 (dd, 1H), 1.76 (s, 2H), 1.56 (s, 3H), 1.42 (s, 6H), 0.80 (s, 9H). MS *m*/*z* 364 (M+H). Anal. Calcd for $C_{23}H_{29}N_3O$: C, 76.00; H, 8.04; N, 11.56. Found: C, 75.94; H, 7.98; N, 11.42.

*3,4-Dimethyl-2-(5-(trifluoromethyl)benzotriazol-2-yl)phenol (**9**).* A light yellow solid (0.36 g, 42%) with a melting point of 127.5−128.5 °C. ^{1}H NMR ($CDCl_3$): δ 8.38 (s, 1H), 8.15 (d, 1H), 7.71 (s, 1H), 7.68 (dd, 1H), 7.25 (d, 1H), 6.96 (d, 1H), 2.35 (s, 3H), 2.27 (s, 3H). MS *m*/*z* 308 (M+H). Anal. Calcd for $C_{15}H_{12}F_3N_3O$: C, 58.63; H, 3.94; N, 13.67. Found: C, 58.66; H, 3.71; N, 13.60.

*2,3-Dimethyl-4-(5-(trifluoromethyl)benzotriazol-2-yl)phenol (**8**).* A white solid (15 g, 46%) with a melting point of 135−136 °C. ^{1}H NMR ($CDCl_3$): δ 8.33 (d, 1H), 8.09 (d, 1H), 7.65 (dd, 1H), 7.31 (d, 1H), 6.78 (d, 1H), 5.30 (broad s, 1H), 2.29 (s, 3H), 2.14 (s, 3H). ^{19}F NMR ($CDCl_3$): −68.9 ppm. Anal. Calcd for $C_{15}H_{12}F_3N_3O$: C, 58.63; H, 3.94; N, 13.67. Found: C, 58.53; H, 3.88; N, 13.72.

*2-(4-Methoxy-2,3-dimethylphenyl)-5-(trifluoromethyl)-2H-benzotriazole (**10**).* A white solid (0.30 g, 27%) with a melting point of 109−111 °C. ^{1}H NMR ($CDCl_3$): δ 8.34 (s, 1H), 8.10 (d, 1H), 7.63 (dd, 1H), 7.42 (d, 1H), 6.88 (d, 1H), 3.92 (s, 3H), 2.27 (s, 3H), 2.15 (s, 3H). MS *m*/*z* 322 (M+H). Anal. Calcd for $C_{16}H_{14}F_3N_3O$: C, 59.81; H, 4.39; N, 13.08. Found: C, 59.65; H, 4.10; N, 13.08.

*2-(6-Methoxy-2,3-dimethylphenyl)-2H-benzotriazole (**11**).* A white solid (0.46 g, 48%) with a melting point of 121.5−122.5 °C. ^{1}H NMR ($CDCl_3$): δ 8.00 (m, 2H), 7.44 (m, 2H), 7.30 (d, 1H), 6.84 (d, 1H), 3.72 (s, 3H), 2.30 (s, 3H), 1.81 (s, 3H). MS *m*/*z* 254 (M+H). Anal. Calcd for $C_{15}H_{15}N_3O$: C, 71.13; H, 5.97; N, 16.59. Found: C, 71.01; H, 5.82; N, 16.75.

*2-Benzotriazol-2-yl-3,4-dimethylphenol (**6**).* A white solid (0.22 g, 17%) with a melting point of 166.5−167.5 °C. ^{1}H NMR ($CDCl_3$): δ 8.04 (s, 1H), 8.00 (m, 2H), 7.51 (m, 2H), 7.21 (d, 1H), 6.95 (d, 1H), 2.34 (s, 3H), 2.32 (s, 3H). MS *m*/*z* 240 (M+H). Anal. Calcd for $C_{14}H_{13}N_3O$: C, 70.28; H, 5.48; N, 17.56. Found: C, 70.02; H, 5.58; N, 17.53.

*4-Benzotriazol-2-yl-2,3-dimethylphenol (**5**).* A light yellow solid (1.79 g, 14%) with a melting point of 189−190 °C. ^{1}H NMR ($CDCl_3$): δ 7.94 (m, 2H), 7.46 (m, 2H), 7.30 (d, 1H), 6.78 (d, 1H), 5.19 (s, 1H), 2.28 (s, 3H), 2.14 (s, 3H). MS *m*/*z* 240 (M+H). Anal. Calcd for $C_{14}H_{13}N_3O$: C, 70.28; H, 5.48; N, 17.56. Found: C, 70.06; H, 5.51; N, 17.65.

*2-(4-Methoxy-2,3-dimethylphenyl)-2H-benzotriazole (**7**).* A white solid (0.17 g, 40%) with a melting point of 110−110.5 °C. ^{1}H NMR ($CDCl_3$): δ 7.94 (m, 2H), 7.44 (m, 2H), 7.41 (d, 1H), 6.85 (d, 1H), 3.91 (s, 3H), 2.28 (s, 3H), 2.14 (s, 3H). MS *m*/*z* 254 (M+H). Anal. Calcd for $C_{15}H_{15}N_3O$: C, 71.13; H, 5.97; N, 16.59. Found: C, 71.03; H, 5.81; N, 16.69.

*2-Benzotriazol-2-yl-4,5-dimethylphenol (**3**).* A white solid (0.15 g, 11%) with a melting point of 143−143.5 °C. ^{1}H NMR ($CDCl_3$): δ 11.04 (s, 1H), 8.14 (s, 1H), 7.95 (m, 2H), 7.46 (m, 2H), 7.01 (s, 1H), 2.32 (s, 3H), 2.31 (s, 3H). MS *m*/*z* 240 (M+H). Anal. Calcd for $C_{14}H_{13}N_3O$: C, 70.28; H, 5.48; N, 17.56. Found: C, 69.98; H, 5.40; N, 17.63.

*2-(6-Methoxy-2,3-dimethylphenyl)-5-(trifluoromethyl)-2H-benzotriazole (**12**).* A light yellow solid (0.35 g, 9%). ^{1}H NMR ($CDCl_3$): δ 8.36 (s, 1H), 8.11 (d, 1H), 7.65 (dd, 1H), 7.35 (d, 1H), 6.86 (d, 1H), 3.72 (s, 3H), 2.31 (s, 3H), 1.81 (s, 3H). MS *m*/*z* 322 (M+H). Anal. Calcd for $C_{16}H_{14}F_3N_3O$: C, 59.81; H, 4.39; N, 13.08. Found: C, 59.58; H, 4.03; N, 13.11.

*4,5-Dimethyl-2-(5-(trifluoromethyl)benzotriazol-2-yl)phenol (**4**).* A light yellow solid (4.02 g, 9%) with a melting point of 113−114 °C. ^{1}H NMR ($CDCl_3$): δ 10.75 (s, 1H), 8.29 (d, 1H), 8.16 (s, 1H), 8.06 (d, 1H), 7.67 (d, 1H), 7.02 (s, 1H), 2.33 (s, 3H), 2.32 (s, 3H). ^{19}F NMR ($CDCl_3$): −68.9 ppm; MS *m*/*z* 308 (M+H). Anal. Calcd for $C_{15}H_{12}F_3N_3O$: C, 58.63; H, 3.94; N, 13.67. Found: C, 58.55; H, 3.79; N, 13.60.

*2-(4-Methoxyphenyl)-2H-benzotriazole (**15**).* A white solid (2.12 g, 24%) with a melting point of 111−112 °C. ^{1}H NMR ($CDCl_3$): δ 8.29 (m, 2H), 7.93 (m, 2H), 7.42 (m, 2H), 7.07 (m, 2H), 3.91 (s, 3H). MS *m*/z 225, 210, 182. Anal. Calcd for $C_{13}H_{11}N_3O$: C, 69.32; H, 4.92; N, 18.65. Found: C, 69.10; H, 4.80; N, 18.65.

Acknowledgment. The authors at Columbia thank the National Science Foundation (Grants CHE-98-12676 and CHE-01-10655) for its generous support of this research. A.J.M. thanks the NSF for a predoctoral fellowship and Drs. Mark Kleinman, Steffen Jockusch, and Tracy Morkin for their comments on the manuscript. We thank the reviewers for their insightful comments and suggestions.

Supporting Information Available: UV−vis and emission spectra for **6** and **3** in DMSO and acetonitrile. Table of optical density of long wavelength (340 nm) absorption band in binary DMSO/acetonitrile solvent system as a function of DMSO. This information is available free of charge via the Internet at http://pubs.acs.org.

References and Notes

(1) Otterstedt, J. *J. Chem. Phys.* **1973**, *58*, 5716.
(2) Decker, C.; Biry, S.; Zahouily, K. *Polym. Degrad. Stab.* **1995**, *42*, 111.
(3) Catalan, J.; Valle, J. D.; Fabero, F.; Garcia, N. *Photochem. Photobiol.* **1995**, *61*, 118.
(4) Weichmann, M.; Port, H.; Frey, W.; Larmer, F.; Elsaesser, T. *J. Phys. Chem.* **1991**, *95*, 1918.
(5) Goeller, G.; Rieker, J.; Maier, A.; Stezowski, J.; Daltrozzo, E.; Neureiter, M.; Port, H.; Wiechmann, M.; Kramer, H. *J. Phys. Chem.* **1988**, *92*, 1452.
(6) Kummrow, A.; Dreyer, J.; Chudoba, C.; Stenger, J.; Nibbering, E. T. J.; Elsaesser, T. *J. Chin. Chem. Soc. (Taipei)* **2000**, *47*, 721.
(7) Weichmann, M.; Port, H. *J. Lumin.* **1991**, *48,49*, 217.
(8) Estevez, C.; Bach, R.; Hass, K.; Schneider, W. *J. Am. Chem. Soc.* **1997**, *119*, 5445.
(9) Flom, S.; Barbara, P. *Chem. Phys. Lett.* **1983**, *94*, 488.
(10) Ghiggino, K.; Scully, A.; Leaver, I. *J. Phys. Chem.* **1986**, *90*, 5089.
(11) Rieker, J.; Lemmert-Schmitt, E.; Goeller, G.; Roessler, M.; Stueber, G.; Schettler, H.; Kramer, H.; Stezowski, J.; Hoier, H.; Henkel, H.; Schmidt, A.; Port, H.; Weichmann, M.; Rody, J.; Rytz, G.; Slongo, M.; Birbaum, J. *J. Phys. Chem.* **1992**, *96*, 10225.
(12) Woessner, G.; Goeller, G.; Rieker, J.; Hoier, H.; Stezowski, J.; Daltrozzo, E.; Neureiter, M.; Kramer, H. *J. Phys. Chem.* **1985**, *89*, 3629.
(13) Frey, W.; Elsaesser, T. *Chem. Phys. Lett.* **1992**, *189*, 565.
(14) Dux, R.; Ghiggino, K.; Vogl, O. *Aust. J. Chem.* **1994**, *47*, 1461.
(15) O'Connor, D.; Scott, G.; Coulter, D.; Gupta, A.; Webb, S.; Yeh, S.; Clark, J. *Chem. Phys. Lett.* **1985**, *121*, 417.
(16) Scully, A.; Bigger, S.; Ghiggino, K.; Vogl, O. *J. Photochem. Photobiol. A* **1991**, *55*, 387.
(17) Weichmann, M.; Port, H.; Laermer, F.; Frey, W.; Elsaesser, T. *Chem. Phys. Lett.* **1990**, *165*, 28.
(18) Woessner, G.; Goeller, G.; Kollat, P.; Stezowski, J.; Hauser, M.; Klein, U.; Kramer, H. *J. Phys. Chem.* **1984**, *88*, 5544.
(19) DeBellis, A.; Iyengar, R.; Kaprinidis, N.; Rodebaugh, R.; Suhadolnik, J. "Proceedings of Service Life Methodologies and Metrologies Symposium"; Service Life Methodologies and Metrologies Symposium, 1999, Monterey, CA.
(20) McGarry, P. F.; Jockusch, S.; Fujiwara, Y.; Kaprinidis, N. A.; Turro, N. J. *Phys. Chem. A.* **1997**, *101*, 764.
(21) Dai, G.; Wu, S.; Sustic, A.; Vogl, O. *Polym. Bull.* **1988**, *20*, 67.
(22) Rettig, W. *Top. Curr. Chem.* **1994**, *169*, 254 and references therein.
(23) Grabowski, Z.; Dobkowski, J. *Pure Appl. Chem.* **1983**, *55*, 245.
(24) Vogel, M.; Rettig, W. *Ber. Bunsen-Ges. Phys. Chem.* **1985**, *89*, 962.
(25) Rettig, W. *Appl. Phys. B* **1988**, *45*, 145.
(26) Elbe, F.; Keck, J.; Fluegge, A.; Kramer, H.; Fischer, P.; Hayoz, P.; Leppard, D.; Rytz, G.; Kaim, W.; Ketterle, M. *J. Phys. Chem. A* **2000**, *104*, 8296.
(27) Keck, J.; Roessler, M.; Schroeder, C.; Stueber, G. J.; Waiblinger, F.; Stein, M.; LeGoumiérec, D.; Kramer, H. E. A.; Hoier, H.; Hénkel, S.; Fischer, P.; Port, H.; Hirsch, T.; Rytz, G.; Hayoz, P. *J. Phys. Chem. B* **1998**, *102*, 6975.
(28) Jovanovic, S.; Tosic, M.; Simic, M. *J. Phys. Chem.* **1991**, *95*, 10824.
(29) Kamiya, M.; Akahori, Y. *Bull. Chem. Soc. Jpn.* **1970**, *43*, 268.
(30) Schuddeboom, W.; Jonker, S. A.; Warman, J. M.; Leinhos, U.; Kuehnle, W.; Zachariasse, K. A. *J. Phys. Chem.* **1992**, *96*, 10809.
(31) Suhadolnik, J.; DeBellis, A.; Hendricks-Guy, C.; Iyengar, R.; Wood, M. "Unexpected Electronic Effects on benzotriazole UV absorber photostability: Mechanistic Implications beyond excited state intramolecular proton transfer"; ACS National Meeting, 2000, Washington, DC.
(32) Bernardi, F.; Olivucci, M.; Robb, M. *Chem. Soc. Rev.* **1996**, *25*, 321.
(33) Solntsev, K.; Huppert, D.; Agmon, N. *J. Phys. Chem. A* **1999**, *103*, 6984.
(34) Acuna, A.; Oton, J. *J. Lumin.* **1979**, *20*, 379.
(35) Dobkowski, J.; Herbich, J.; Galievsky, V.; Thummel, R.; Wu, F.; Waluk, J. *Ber. Bunsen-Ges. Phys. Chem.* **1998**, *102*, 469.
(36) Nau, W.; Greiner, G.; Rau, H.; Olivucci, M.; Robb, M. *Ber. Bunsen-Ges. Phys. Chem.* **1998**, *102*, 486.
(37) Shizuka, H. *Acc. Chem. Res.* **1985**, *18*, 141.
(38) Werner, T. *J. Phys. Chem.* **1979**, *83*, 320.
(39) Woessner, G. Photophysikalische und photochemische Desaktivierungsprozesse der UV−Stabilisatoren des Benzotriazol-Typs. Doctoral thesis, University of Stuttgart, 1983.
(40) Kosower, E. *J. Am. Chem. Soc.* **1957**, *80*, 3253.
(41) Kosower, E. *J. Am. Chem. Soc.* **1957**, *80*, 3261.
(42) Stueber, G.; Kieninger, M.; Schettler, H.; Busch, W.; Goeller, B.; Franke, J.; Kramer, H.; Hoier, H.; Henkel, S.; Fischer, P.; Port, H.; Hirsch, T.; Rytz, G.; Birbaum, J. *J. Phys. Chem.* **1995**, *99*, 10097.

(43) Liptay, W. *Angew. Chem., Int. Ed.* **1969**, *8*, 177.

(44) Onsager, L. *J. Am. Chem. Soc.* **1936**, *99*, 1486.

(45) Rettig, W.; Braun, D.; Suppan, P.; Vauthey, E.; Rotkiewicz, K.; Luboradzki, R.; Suwinska, K. *J. Phys. Chem.* **1993**, *97*, 13500.

(46) Michl, J. *J. Mol. Photochem.* **1972**, *4*, 243.

(47) Sinicropi, A.; Pischel, U.; Basosi, R.; Nau, W.; Olivucci, M. *Angew. Chem., Int. Ed.* **2000**, *39*, 4582.

(48) Nau, W.; Greiner, G.; Wall, J.; Rau, H.; Olivucci, M.; Robb, M. *Angew. Chem., Int. Ed.* **1998**, *37*, 98.

(49) Compound **6** (OD >2 absorbance units) was irradiated at 300 nm. The loss rate measured in neat acetonitrile was >0.7 absorbance units/hour. In 3:1 acetonitrile/DMSO the loss rate drops to 0.16 absorbance units/hour. Tinuvin P, under identical conditions, showed a loss rate of 0.08 absorbance units/hour in acetonitrile, and >0.7 abs. units/hour in 3:1 acetonitrile/DMSO.